Remote Sensing of Environment 222 (2019) 232–243

Contents lists available at ScienceDirect

Remote Sensing of Environment

journal homepage: www.elsevier.com/locate/rse

Temporal-spatial differences in lake water storage changes and their links to climate change throughout the Tibetan Plateau

Baojin Qiao[a,b,*], Liping Zhu[b,c,d,**], Ruimin Yang[b,e]

[a] Institute of Smart City, Zhengzhou University, Zhengzhou 450001, China
[b] Key Laboratory of Tibetan Environment Changes and Land Surface Processes, Institute of Tibetan Plateau Research, Chinese Academy of Sciences (CAS), Beijing 100101, China
[c] CAS Center for Excellence in Tibetan Plateau Earth Sciences, Beijing 100101, China
[d] University of Chinese Academy of Sciences, Beijing 100049, China
[e] College of Earth Environmental Sciences, Lanzhou University, Lanzhou 730000, China

ARTICLE INFO

Keywords:
Lake water storage
Tibetan Plateau
Remote sensing
Glacial meltwater
Precipitation

ABSTRACT

Change in lake water storage is an important factor influencing hydrological cycle, regional environment, and climate on the Tibetan Plateau (TP) because of the large number (> 1000 lakes) and huge areas (> 46,500 km^2) of lakes. Due to the lack of in situ lake level monitoring for most lakes, and long-term continuous satellite altimetry data for some large lakes, estimates of water storage changes for all lakes throughout the TP over a long time is challenging. We have estimated the lake water storage changes of 315 lakes (each lake is > 10 km^2) during the period of 1976–2013 through an empirical equation based on Shuttle Radar Topography Mission (SRTM) DEM (Digital Elevation Model) data and Landsat images. These lakes are located within endorheic basins and occupied approximately 80% of the total lake surface areas of the TP in 2013 based on the results of this study and Zhang et al. (2014). The results showed that the lake water storage decreased by 23.69 Gt from 1976 to 1990 and increased by 140.8 Gt from 1990 to 2013. Increased water storage was mainly concentrated in the central TP (regions A) and northern TP (region B). The increase in total lake surface area during the period 2000–2013 in region B (1981.6 km^2) was greater than that in region A (1869.1 km^2), but the increase in the water storage in the former was half of that in the latter, indicating that lake surface area changes cannot represent the degree of lake water storage change due to differences in the topography and lake size. Although the total variation in the rate of the lake water storage change (7.19 Gt/y) was similar to the rate of increase in the mass (7 ± 7 Gt/y) estimated from Gravity Recovery and Climate Experiment (GRACE) data for the whole region, the spatial distribution of these variations was largely different. During the period 2000–2013, a trend analysis revealed that precipitation was perhaps the primary reason for lake change throughout the TP, while a decreasing evaporation rate only contributed approximately 1.5%, 2.5% and 1.7% to the expansions of the lakes in regions A, C and D respectively. However, based on modern glacier mass balance observation data, we estimated that glacial meltwater may have contributed 22.2%, 39.8%, 50.6% and 100% to the increasing water storage during the period 2000–2013 by rough estimates in regions A, B, C and D, respectively, indicating that glacial meltwater perhaps was a primary contributor to lake expansion in region D, which was located in an extremely cold and dry climate with a broad distribution of glaciers.

1. Introduction

The Tibetan Plateau (TP), which is the largest and highest plateau in the world, is the headstream region of many large rivers that nourish hundreds of millions of people throughout Asia. Numerous lakes, which are distributed throughout the TP, especially in the inner TP, e.g., Selin Co and Nam Co, are important components of the water cycle, and thus, changes in these lakes could influence the regional environment and climate. According to recent investigations of lakes in the Tibetan area, 1171 lakes (> 1 km^2) with a total area of 4.65×10^4 km^2 are located throughout the TP (Wan et al., 2016). Most of the lakes on the TP have expanded over the past few decades based on remote sensing images and satellite elevation data, but the southern TP is an exception, where the lakes exhibited shrinking trends (Li et al., 2014; Song et al., 2013;

* Correspondence to: B. Qiao, Institute of Smart City, Zhengzhou University, Zhengzhou 450001, China.
** Correspondence to: L. Zhu, CAS Center for Excellence in Tibetan Plateau Earth Sciences, Beijing 100101, China.
E-mail addresses: qiaobaojin@zzu.edu.cn (B. Qiao), lpzhu@itpcas.ac.cn (L. Zhu).

https://doi.org/10.1016/j.rse.2018.12.037
Received 12 October 2017; Received in revised form 23 November 2018; Accepted 30 December 2018
Available online 09 January 2019

Wan et al., 2014; Wang et al., 2013; Zhang et al., 2011b, 2014; Yang et al., 2017). The expansion of the lakes floods pastures, and consequently, this expansion represents a serious impact on the local economy, environment and ecology.

Glaciers on the TP have experienced substantial shrinkage over the past few decades, especially in the Himalaya (Neckel et al., 2014; Wei et al., 2014; Yao et al., 2012). The results from the study by Neckel et al. (2014) also indicate that most glaciers on the TP showed serious mass reductions based on ICESat (Ice, Cloud and Land Elevation Satellite) and SRTM (Shuttle Radar Topography Mission) data. Based on geometric dependency of the relationships among the lakes, rivers and glaciers, lakes on the TP are more or less dependent on glacial meltwater (Phan et al., 2013). Increasing glacial meltwater with rising temperatures constitutes an important influence on the expansion of lakes and perhaps represents the main cause of lake expansion (Zhang et al., 2011b). The results of Lei et al. (2017) indicate that glacial meltwater was the main reason for lake expansion, as lakes exhibiting dramatic increases during both the warm and cold seasons. A comparison of the differences in water storage changes between glacier-fed and non-glacier-fed lakes in the regions of Tanggula Mountains and northwestern TP (Qiao and Zhu, 2017; Song and Sheng, 2016), showed that glacial meltwater and precipitation-evaporation contributed equally to lake expansion. However, due to the lack of reliable observation data, quantifying both the glacier mass balance for all of the glaciers throughout the TP and the contribution from glacial meltwater to the lakes is difficult. Precipitation has increased over the past few decades, especially in the central TP (Xu et al., 2008). Moreover, the amount of precipitation showed a good relationship with observed changes within lakes, and thus, increasing precipitation was considered to be the main cause of lake expansion (Lei et al., 2013; Liu et al., 2009; Song et al., 2014). The results of hydrological modeling also suggested that precipitation was the main driving factor for lake change (Biskop et al., 2016; Zhou et al., 2016). However, permafrost degradation was also considered to contribute a greater proportion to lake expansion on the TP due to the large water volume released under warming climatic conditions (Li et al., 2014). Lake water surface evaporation is the only mechanism for lake water to be reduction in a closed lake. Increasing evaporation will take much more water out from the lake, whereas decreasing evaporation will reduce water loss from the lake. The significant decrease in evaporation over the Nam Co is considered to be responsible for approximately 4% of lake expansion from 1998 to 2008 (Ma et al., 2016). By quantifying the change of lake water storage, terrestrial water storage, glacier mass, snow water equivalent, soil moisture and permafrost, the contributions of increased net precipitation, glacier mass loss and permafrost degradation to lake expansion were determined to be 74%, 13% and 12%, respectively (Zhang et al., 2017). Therefore, the main cause for lake expansion throughout the TP is still debated due to the lack of both in situ observation data and complete coverage of satellite data.

Previous studies mainly have focused on lake surface area changes under different climatic conditions based on remote sensing images, but area changes cannot fully reflect lake responses to climate changes because of differences in the topography surrounding the lakes. For example, although increases or decreases in the areas of the two lakes may be equal, large difference may be observed in their water storage amounts due to differences in the sizes of those two lakes and the topography around them. On the one hand, only few lake level observation data form several gauging stations (e.g., at the Nam Co, Yamzho Yumco and Qinghai Lake) can be used to estimate water storage changes; on the other hand, bathymetric data for most lakes, which could also be used to estimate water storage and their changes, were still lacking and can only be applied to some large lakes, such as Guozha Co and Nam Co (Qiao et al., 2017; Zhu et al., 2010).

The accuracy of ICESat data is higher than that of other satellite altimetry data, and thus, ICESat data have been widely utilized to estimate water storage changes (Song et al., 2013; Zhang et al., 2011b, 2013a, 2013b). Zhang et al. (2013b) calculated changes in the water storage for 117 lakes in the inner TP, the results of which showed that the total lake water storage change (4.28 Gt/y) explained 61% of the mass increase (7 ± 7 Gt/y) derived from GRACE data by Jacob et al. (2012). Accordingly, they hypothesized that the overall lake water storage changes could approximately account for the total increase in the mass. The results of Song et al. (2013) showed that the total amount of lake water storage increased by 81.34 km^3 (6.79 km^3/y) from 2000 to 2011 based on ICESat data and modeling, the results of which are consistent with the increased mass (54.5 km^3 at a rate of 6.81 km^3/y) observed from 2003 to 2010 that were derived from GRACE data. Therefore, increased mass in the inner TP may be attributable to the lake expansion based on the relationship between lake water storage and mass (Jacob et al., 2012; Song et al., 2013; Zhang et al., 2013b). Although the signals within the GRACE data fundamentally consist of regional soil moisture, glacier ice, snow water equivalent, lake water, permafrost and groundwater storage estimates (Xiang et al., 2016), these factors only cycled within the region if they were changed by precipitation and evaporation. Therefore, precipitation was considered the main reason for the lake expansion.

Lake level change is important metric in studies of lake water storage change. However, only a few large lakes have long periods of satellite image coverage based on the ICESat and Cryosat-2 data (Jiang et al., 2017; Zhang et al., 2011b), and the estimation of total lake water storage change remains uncertain. As a consequence, a comprehensive investigation of lake water storage changes throughout the TP over a long time needs to be performed. SRTM, which provides reliable topographic data throughout the TP, can be used to estimate lake water storage change based on lake surface area and lake level variation. In this study, we have investigated the water storage changes in 315 lakes (each of them was > 10 km^2 in 2013) for the period from 1976 to 2013 based on SRTM data and Landsat images. These lakes are located in endorheic basins (Fig. 1) and possess approximately 80% of the total areas of the lakes on TP. To analyze the spatial difference in the water storage changes, we divided the study region into five regions: A, B, C, D and E (Fig. 1) based on the size of the lake, the lake water storage change and the basin boundary according to HydroSHEDS. The detailed principles and methods of the regional division are shown in Section 2.5. The purpose of this study was to (1) estimate water storage change over a long time, (2) analyze the spatial differences in the water storage changes, and (3) analyze the potential link between lake expansion and climate change.

2. Method and data

2.1. Multi-temporal Landsat images for extracting the lake surface area

Landsat Multispectral Scanner (MSS), Thematic Mapper (TM), Enhanced Thematic Mapper Plus (ETM+) and Operational Land Image (OLI) images were used to extract the lake surface areas for 1976, 1990, 2000, 2005 and 2013, and a total of 242 images were downloaded from the U.S. Geological Survey (USGS) website (http://glovis.usgs.gov/) and the Geospatial Data Cloud, Computer Network Information Center, Chinese Academy of Sciences website (http://www.gscloud.cn/). In addition, we also used 2 images from 1977 and 18 images from the other years (1989, 1991, 2001, 2004, 2006 and 2014, 3 images for each year) to supplement the lack of images in the neighboring years. To reduce the influences of seasonal variations, the highest quality images were selected between September and November, which is the period with the least cloud and snow cover. The method of Normalized Difference Water Index (NDWI), introduced for multiple purposes by different authors in 1996. McFeeters (1996) used the NDWI index to extract water bodies, and Gao (1996) used it to delineate the amount of water present in vegetation. In this paper, we use this method to extract the lake boundaries, and following the relationship $NDWI = (Green - NIR) / (Green + NIR)$, where Green denotes the

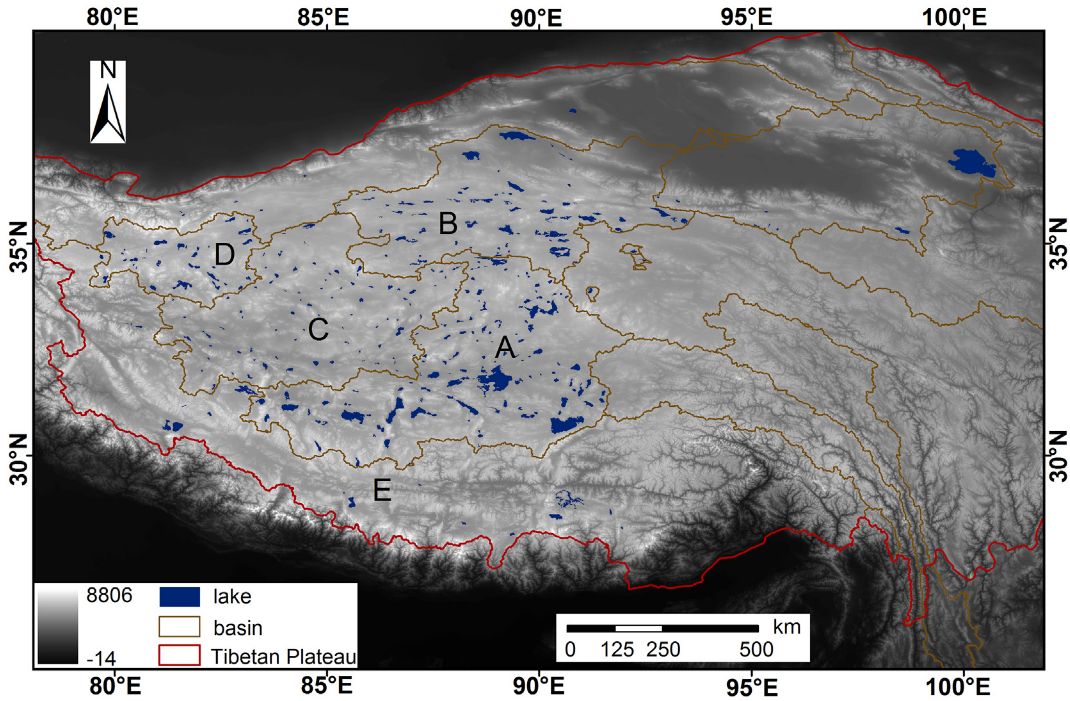

Fig. 1. The distribution of lakes throughout the TP.

green band and NIR is the near infrared band. This method classifies the lake, and a portion of glacier and the mountain shadow into a single class. The boundary extraction accuracy being controlled by the pixel dimension (30 m). All data were projected into Albers Conical Equal Area coordinate system.

The first step of NDWI is to process the image by radiometric correction; the band ratio method is used, with NDWI = (Green − NIR) / (Green + NIR), and the range of the color slice with 0–1 is chosen to extract the water body boundary. The above steps are processed by ENVI software. Finally, the error boundary is modified by manual interpretation in ArcGIS software.

2.2. Estimating water storage change based on SRTM

The SRTM acquired digital elevation model (DEM) data spanning > 80% of the globe during an eleven-day mission in February 2000. The absolute vertical and horizontal precision of the SRTM data within a 90 m grid is 16 m and 20 m, respectively. However, the absolute height error of the SRTM data varies globally from 5.6 to 9.0 m with an error of 6.2 m in Asia (Rodriguez et al., 2006), so the actual performance of the SRTM data was much better than the expected results. Because most of the lake levels throughout the TP have risen since 2000, and topographic data surrounding the lakes have been available since 2000 according to the SRTM, so that the relationship between lake surface area and lake surface elevation can be established. The results of Song et al. (2013) indicate that the water level and surface area have a good relationship, according to a Pearson's correlation coefficient of 0.964 at a confidence level of 99%, obtained from the analysis of 13 data point pairs, and to estimate lake water storage change obtained from the linear relationship between the lake surface area and water level. Thus, this method can be used to estimate the water storage changes through an empirical equation concerning lake surface area and lake level changes. To verify the accuracy of the method with the SRTM to estimate lake water storage change, Yang et al. (2017) calculated lake water storage change based on bathymetric data of five lakes of different size (Nam Co was largest, with an area of 2020.9 km^2, and Gyado Co was smallest, with an area of 42.72 km^2), and these results were regarded as "true value", including the results of lake water storage change below the surface in 2000, in which the topography was unknown with using the SRTM method, the results showed that the average error in the method using SRTM was 4.98%, indicating that this method of using SRTM to estimate lake water storage change was considered reliable. We used the same method as Yang et al. (2017) to estimate the water storage changes.

For example, the Nam Co lake level showed a continuously increasing trend over the past few decades (Wu et al., 2014; Zhang et al., 2011a; Zhu et al., 2010), and the lake levels in 2005 and 2013 were much higher than in 2000. DEM data of Nam Co basin were extracted based on the basin boundaries from HydroSHEDS (Hydrological data and maps based on Shuttle Elevation Derivatives at multiples Scales) database, which provides hydrographic information (e.g., stream networks, watershed boundaries and drainage directions) for regional and global-scale applications (Lehner et al., 2008). Then, the DEM data (raster data) were converted into polygon data (vector data) with elevation values. Areas having the same elevation value were dissolved together by ArcGIS 9.3, so that the area of each elevation value could be calculated (Table 1). For example, 4724 m represents the lake surface, to sum the area of all 4724 m is the lake surface area. Calculating the lake surface area and lake surface elevation of Nam Co, and a series of values were showed in Table 1, and Pearson's correlation coefficient between lake surface area and lake level was 0.998 at a confidence level of 99%.

When the lake surface area and lake surface elevation data were known for two periods (second and third column of Table 1), water storage change with 1 m interval (fourth column of Table 1) was estimated based on the empirical equation (Eq. (1)); and by summing all the water storage change of 1 m interval between this period to 4724, lake water storage change of this period relative to 2000 (4724 m) was also known (fifth column of Table 1). For example, lake water storage of 4727 m to 4724 m (5.979 km^3) is to sum water storage changes with 1 m intervals of 4725 to 4724 (1.98 km^3), 4726 to 4725 (1.992 km^3) and 4727 to 4726 (2.007 km^3). After this determination, a linear relationship between the lake surface area and lake water storage change was established based on the third and fifth column of Table 1 (Fig. 2b). Water storage change could be estimated relative to 2000 when the area was known based on the linear relationship.

Table 1
The relationship between the lake surface area and elevation from SRTM.

Elevation (m)	Area of each elevation value (km^2)	Lake surface area (km^2)	Water storage change with1 m interval (km^3)	Water storage change relative to 4724 m (km^3)
4724	1974.6	1974.6	0	0
4725	9.9944	1984.594	1.980	1.980
4726	14.4025	1998.997	1.992	3.971
4727	16.5538	2015.551	2.007	5.979
4728	16.9055	2032.456	2.024	8.003
4729	17.8903	2050.347	2.041	10.044
4730	18.3827	2068.729	2.060	12.104
4731	18.5116	2087.241	2.078	14.182
4732	18.1365	2105.377	2.096	16.278
4733	17.4975	2122.875	2.114	18.392
4734	17.0931	2139.968	2.131	20.523
4735	20.915	2160.883	2.150	22.674
4736	19.4378	2180.321	2.171	24.844
4737	19.5081	2199.829	2.190	27.034
4738	19.215	2219.044	2.209	29.244
4739	20.024	2239.068	2.229	31.473
4740	19.9067	2258.975	2.249	33.722
4741	22.3511	2281.326	2.270	35.992
4742	24.2972	2305.623	2.293	38.286
4743	24.3852	2330.008	2.318	40.603
4744	23.1307	2353.139	2.342	42.945

$$\Delta V = \frac{1}{3} \times (S_1 + \sqrt{S_1 \times S_2} + S_2) \times \Delta h \tag{1}$$

where S_1 and S_2 represent the lake surface areas of the two periods, $\triangle h$ represents the lake level change during the two periods, and $\triangle V$ represents the water storage change during the two periods.

2.3. CMFD dataset for investigating precipitation and temperature variations

The China Meteorological Forcing Dataset (CMFD) was developed by the Institute of Tibetan Plateau Research, Chinese Academy of Sciences (He and Yang, 2011). This dataset spans the period during 1979–2013, and merges the meteorological data from 740 operational stations of the China Meteorological Administration (CMA) into Princeton meteorological forcing data (Sheffield et al., 2006), and the Tropical Rainfall Measuring Mission (TRMM) 3B42 precipitation products (Huffman et al., 2007) to produce near-surface temperature, pressure, wind speed, and specific humidity and so on, the temporal and spatial resolutions are 3 h and 0.1°, respectively. These data have been widely utilized for climate studies throughout the TP (Chen et al., 2011; Liu and Xie, 2013; Yang et al., 2013, 2016; Zhou et al., 2016). Precipitation and temperature variations during the study period from 1979 to 2013 were obtained from the CMFD dataset.

2.4. Estimation of evaporation changes over the TP

Lake surface evaporation is an important factor that influences lake changes. However, actual evaporation data are lacking, and meteorological stations are sparse throughout the TP. The Penman equation (Penman, 1948) has been widely and successfully used to calculate open-water evaporation rate around the globe (McMahon et al., 2013). Thus, we used this method to calculate the Ep for 57 meteorological stations throughout the TP, and the Kriging interpolation method was used to estimate the spatial and temporal distribution of the Ep over the TP. The daily maximum and minimum temperature, relative humidity, sunshine duration and wind velocity data were used to calculate the Ep from 1976 to 2013.

$$\mathrm{Ep} = \frac{\Delta}{\Delta + \gamma}\frac{\mathrm{Rn}}{\lambda} + \frac{\gamma}{\Delta + \gamma}\frac{6430\,(1 + 0.536\mathrm{u2})\mathrm{D}}{\lambda} \tag{2}$$

where Rn is the daily net radiation (MJ m^{-2} day^{-1}), $\triangle$ is the slope of the saturation vapour pressure curve (kPa/°C), γ is the psychrometric constant (kPa/°C), D is the vapour pressure deficit (Pa), u_2 is daily average wind speed at 2 m height (m/s), and λ is the latent heat of vaporization of water (2.45×10^6 J/kg).

The complete ice cover of Hoh Xil lakes was completed sometime between the middle of October and the early December, and the complete melt was completed between the early May and the middle of June based on MODIS and Landsat images (Yao et al., 2015). The lake surface was covered by ice during the low temperatures of winter, so sublimation from the lake surface ice could be considered negligible (Ma et al., 2016). We assume that the Ep value for May to November could represent the annual Ep, with Ep value of December to April being 0.

2.5. Principles and methods of regional division

To analyze the spatial difference of water storage change, we divided the study region into several sub-regions based on the lake size, lake water storage change and basin boundary. The lake size and lake water storage change of these lakes, which are located in the southern and eastern part of study region, are greatest among all the lakes, such as Nam Co, Selin Co, Zharinanmu Co and Tangra Yumco; we divided these lakes into a sub-region, named region A. The lake size and lake water storage change of the lakes located in the northern part of study region designated as region B, are smaller than the lakes of region A. The lakes located in the central part of study region, whose lake size and water storage change are smallest among all the lakes, are designated as being region C. Region D has lakes that are in an area that is extremely cold and has a dry climate conditions, with a broad

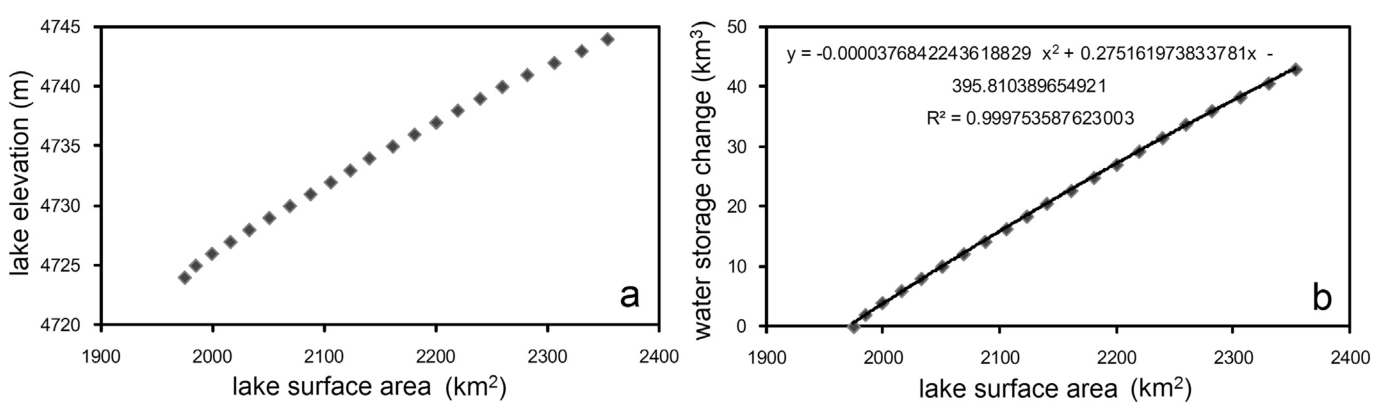

Fig. 2. The relationships among the lake elevation, lake surface area and water storage changes. a, The relationship between the lake surface area and lake elevation; b, the relationship between the lake surface area and water storage changes.

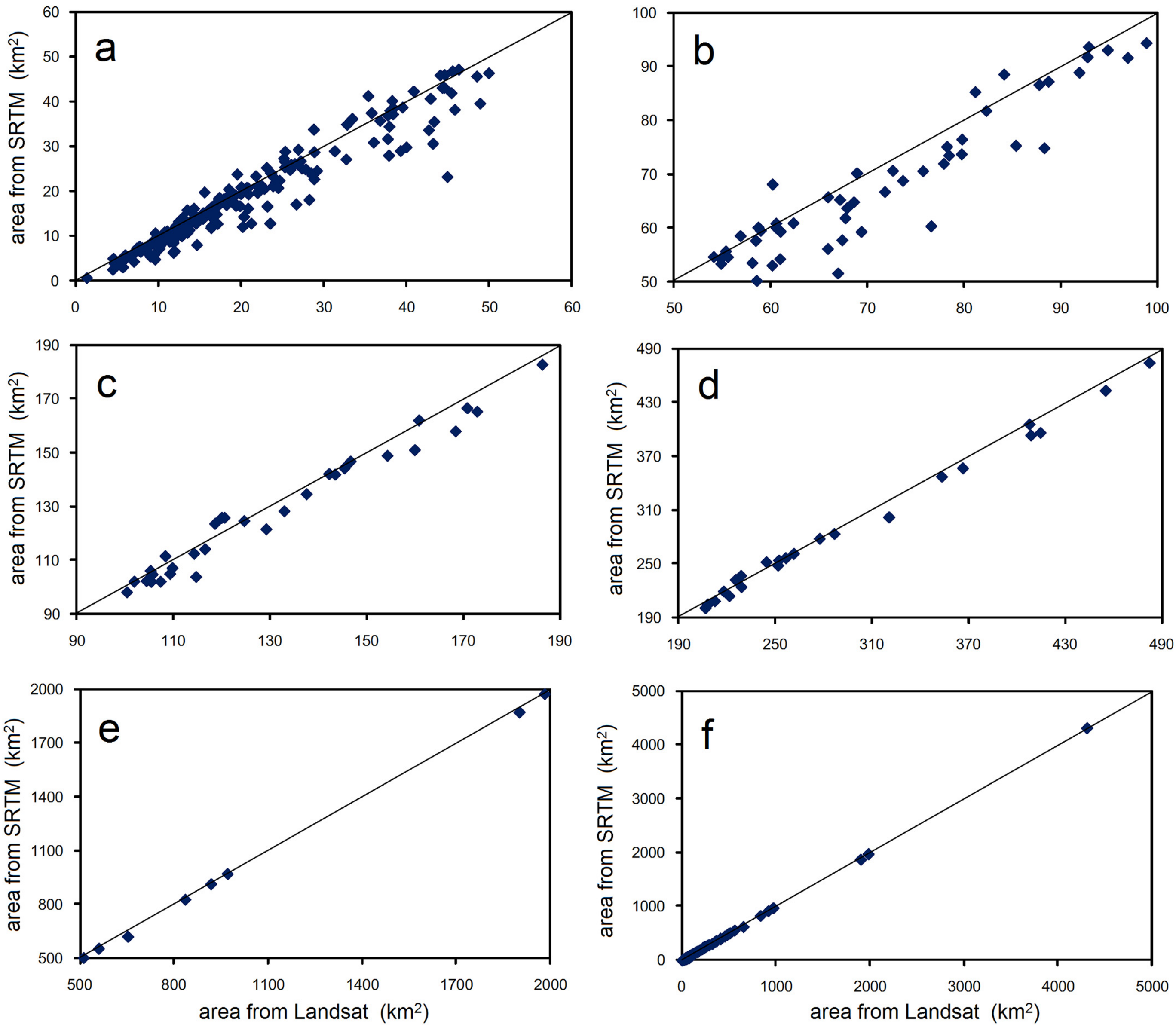

Fig. 3. Comparison of lake surface areas derived using SRTM data and Landsat images for different lake sizes: a, 0–50 km^2; b, 50–100 km^2; c, 100–200 km^2; d, 200–500 km^2; e, 500–2000 km^2; f, all lakes.

distribution of glaciers, and the lake sizes and water storage changes are larger than observed in region C. Region E contains several lakes, which are located in the southern part of the study region, and these lakes are experiencing a trend toward shrinkage.

3. Results

3.1. Assessment of the precision of SRTM

Because the elevations of the lake surface are relatively invariable, we were able extract the area of the lake using the SRTM data based on the similar lake surface elevation values; for example, the SRTM-based elevation of Nam Co was 4724 m in 2000 with an area of 1974.6 km^2, which is similar to the value of 1981.2 km^2 in the Landsat image from 2000. The areas of all the lakes in 2000 were subsequently calculated using the SRTM data. As shown in Fig. 3, we separated the lakes into six categories, 0–50 km^2 (Fig. 3a), 50–100 km^2 (Fig. 3b), 100–200 km^2 (Fig. 3c), 200–500 km^2 (Fig. 3d), 500–2000 km^2 (Fig. 3e) and all lakes (Fig. 3f). The results demonstrated good consistency between the areas derived using SRTM and those from Landsat images with high correlations of 0.959, 0.885, 0.977, 0.997, 1.00 and 1.00 for the six categories, most of which were distributed around the 1:1 line. The larger lakes (> 100 km^2) were much closer to the1:1 line than the smaller lakes, indicating that the SRTM data exhibited a high height precision and a better performance for the larger lakes than the smaller lakes. A comparison of the SRTM results with the bathymetric results used to estimate the water storage changes for the five lakes revealed an average relative error of only 4.98% (Yang et al., 2017). In this study, only the relative elevation changes were employed to estimate the water storage changes, and thus, the SRTM data were sufficiently reliable for this research.

3.2. Lake surface area and water storage change

A total of 315 lakes (> 10 km^2) were investigated in this study. The areas of the five largest lakes, including Qinghai Lake (4362.9 km^2), Selin Co (2397.4 km^2), Nam Co (2020.9 km^2), Duoersuodong Co (1056.9 km^2) and Zharinam Co (1001.6 km^2), were larger than

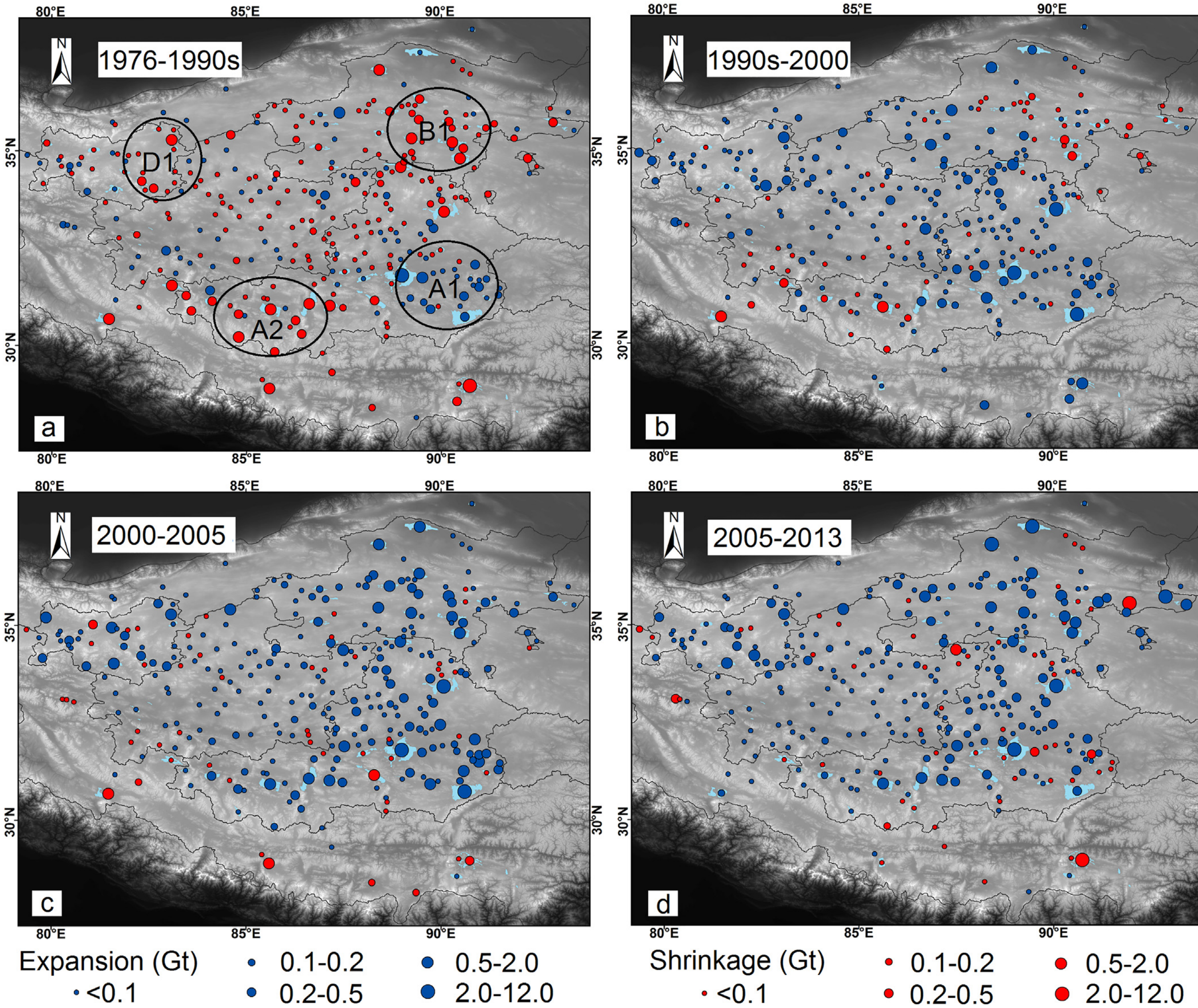

Fig. 4. Lake water storage changes in the different regions from 1976 to 2013.

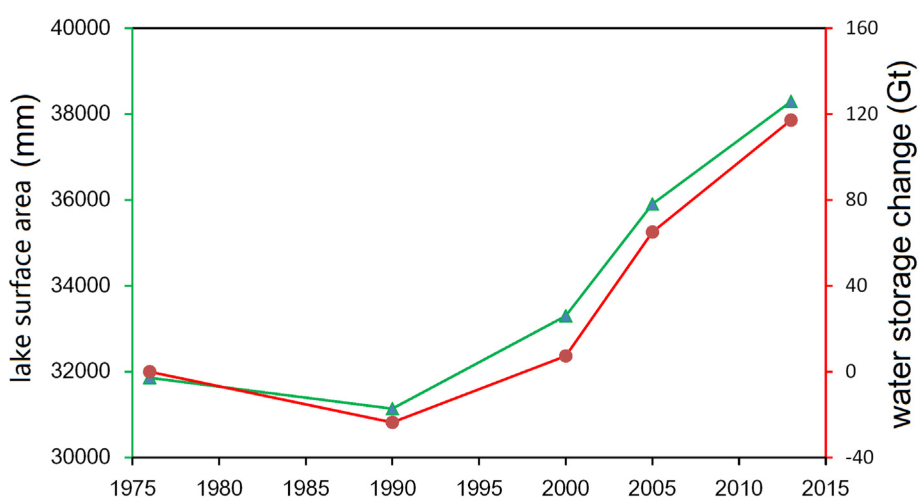

Fig. 5. Total lake surface area and water storage changes from 1976 to 2013.

1000 km^2 in 2013. Four of these five lakes were located in region A, except Qinghai Lake. Most lakes are distributed throughout regions A and B. By region, 113 lakes are in region A, 60 are in region B, 79 are in region C, 30 are in region D (including Gozha Co, Longmu Co and Bangdag Co), and 17 are in region E (including Yamzho Yumco and Lake Manasarovar). The total lake surface areas in 2013 throughout regions A, B, C, D and E were 17,111.67 km^2, 7209.95 km^2, 2878.65 km^2, 2821.28 km^2 and 2688.74 km^2, respectively.

As shown in Fig. 4a, most of the lakes demonstrated shrinking trends from 1976 to 1990 except for some lakes around Selin Co and Nam Co. The total area and water storage of the 315 lakes decreased by 721.95 km^2 (51.56 km^2/y) and 23.69 Gt (1.69 Gt/y), where 1 Gt = 1 km^3 with an assumption that the density of lake water is 1000 kg/m^3. This trend was especially true in Qinghai Lake, the area of which decreased by 182.8 km^2 with a water storage reduction of 8.05 Gt, but the area and water storage of Selin Co increased by 99.34 km^2 and 2.85 Gt, respectively. Except for some lakes in the western parts of region A and region B, most lakes expanded after 1990. The total area and water storage increased by 2159.5 km^2 (216 km^2/y) and 31.02 Gt (3.1 Gt/y) from 1990 to 2000, respectively, by 2608.76 km^2 (521.75 km^2/y) and 57.67 Gt (11.53 Gt/y) from 2000 to 2005, respectively, and by 2388.27 km^2 (298.53 km^2/y) and 52.13 Gt (6.51 Gt/y) from 2005 to 2013, respectively. Evidently, the lake expansion rate was much faster during 2000–2005 than during the other periods.

As shown in Fig. 5, the total lake surface area increased from 1976 (31,858.04 km^2) to 2013 (38,292.63 km^2) at an average rate of 173.9 km^2/y, and the water storage increased by 140.8 Gt. However, the total lake surface area and water storage decreased by 721.9 km^2 and 23.7 Gt, respectively, from 1976 to 1990. Subsequently, the lakes started to expand, with respective increases in the lake surface area and water storage of 2159.5 km^2 and 31 Gt from 1990 to 2000, of 521.8 km^2 and 57.7 Gt from 2000 to 2005, and of 298.5 km^2 and 52.1 Gt from 2000 to 2013. The increased lake surface area from 1990 to 2000 (2159.5 km^2) was approximately 4 times that from 2000 to 2005 (521.8 km^2), but the increased water storage (31 Gt) was only one half that from 2000 to 2005 (57.8 Gt). The increased lake surface area from 2000 to 2005 (521.8 km^2) was approximately 1.7 times that from 2005 to 2013 (298.5 km^2), but the increased water storage (57.8 Gt) was nearly the same as that from 2000 to 2005 (52.1 Gt). These results indicate that the lake surface area and water storage changes were not consistent and that variations in the water storage could represent real change in the lake due to the different lake sizes and different regional topography profiles.

The detailed lake surface area and water storage changes in each region are shown in Table 2. Although the areas of regions A and C increased by 100.9 km^2 and 8.63 km^2, respectively, the water storage for all five regions showed shrinking trends from 1976 to 1990. After 1990, most of the lakes expanded and the water storage changes were mainly concentrated in regions A and B (Fig. 4). The water storage of region A increased by 19.21 Gt from 1990 to 2000, but the water storage in regions B, C and D increased by only 2.29 Gt, 4.15 Gt and 3.4 Gt, respectively. The water storage in region E increased by only 1.8 Gt during the period 1990–2000, whereas it shrank in the other periods. Lake water storage in regions A and B, which increased by 59.02 Gt (4.54 Gt/y) and 29.7 Gt (2.28 Gt/y) from 2000 to 2013, occupied 53.75% and 27.05% of total increasing water storage, respectively. Among these lakes, 263 lakes showed an increasing water storage trend of 122.02 Gt (9.39 Gt/y), and the water storage of 52 lakes decreased by 12.21 Gt (0.94 Gt/y) from 2000 to 2013.

For an individual lake, the largest water storage change was Selin Co which increased by 2.85 Gt from 1976 to 1990, 4.87 Gt from 1990 to 2000, 11.52 Gt (2.3 Gt/y) from 2000 to 2005 and 6.71 Gt (0.84 Gt/y) from 2005 to 2013. Water storage of Nam Co only increased by 0.36 Gt from 1976 to 1990, 3.95 Gt from 1990 to 2000, 4.63 Gt (0.93 Gt/y) from 2000 to 2005 and 0.33 Gt (0.04 Gt/y) from 2005 to 2013. Lake Qinghai decreased by 2.27 Gt (0.45 Gt/y) from 2000 to 2005, and then increased by 4.53 Gt (0.57 Gt/y) from 2005 to 2013. The largest shrinkage was Yamzho Yumco in region E which had decreased by 0.23 Gt (0.05 Gt/y) from 2000 to 2005, and then by 2.76 Gt (0.34 Gt/y) from 2005 to 2013.

3.3. Related climate elements change during the studied period

The precipitation in region A was much greater than that of the other regions during 1979–2013, and the precipitation showed a decreasing trend from 1979 to 1994 (Fig. 6a). However, the other three regions demonstrated minor variations during this period (Fig. 6a). The precipitation increased rapidly after 1994, and the average precipitation quantities in regions A, B, C and D were 283.85 mm, 117.65 mm, 137.47 mm and 61.16 mm, respectively, during 1979–1993, and 321.53 mm, 198.16 mm, 184.64 mm and 138.3 mm, respectively, during 1994–2013. The Ep showed a similarly increasing trend among the four regions from 1984 to 2000, followed by a decreasing trend from 2000 to 2009. Increasing Ep trends were observed among all of the regions from 1976 to 2000, after which the Ep value began to decrease. The Ep in region B was the lowest, with an average of 1296.8 mm/y among the four regions. Regions C and D exhibited the highest Ep value of 1364.1 mm/y and 1361.1 mm/y, respectively, and region A had an Ep value of 1341.3 mm/y (Fig. 6b). We used linear regression to calculate the tendency for increase or decrease, student's *t*-test was used to assess the significance of the trends, and only those with a P value < 0.05 were considered as statistically significant, the results indicated that the rates of decrease in the Ep were −4 mm/y ($P < 0.05$), −4.6 mm/y ($P < 0.05$) and − 5.3 mm/y ($P < 0.05$) for regions A, C and D, respectively, from 2000 to 2013. The temperature distributions among the four regions showed a significantly increasing trend except for region B, where it decreased from 2005 to 2013 (Fig. 6c). The average temperature of region A was −3.17 °C which was the highest among the four regions, while those for regions B and C were −6.3 °C and 5.06 °C, respectively, and the average temperature for region D was −11.17 °C, which was the lowest. Low precipitation and temperature conditions with high Ep value suggest that region D was located in an extremely cold and dry climate, while high precipitation and temperature conditions with low Ep values indicated that region A was located in a warm and moist climate.

Table 2
Lake surface area and water storage change in each region.

Period	Region A		Region B		Region C		Region D		Region E	
	AC(km^2)	WSC(Gt)	AC(km^2)	WSC(Gt)	AC(km^2)	WSC(Gt)	AC(km^2)	WSC(Gt)	AC(km^2)	WSC(Gt)
1976–1990s	100.9	−3.02	−487.44	−4.86	8.63	−0.49	−83.69	−1.87	−55.45	−4.59
1990s–2000	755.54	19.21	457.26	2.29	650.82	4.15	163.72	3.4	91	1.8
2000–2005	1235.98	36.46	1068.04	14.68	242.57	4.08	160.3	6.32	−96.87	−2.7
2005–2013	633.15	22.57	910.58	15.02	243.53	2.89	312.86	5.45	−57.75	−3.29
Sum	2725.56	75.21	1948.44	27.13	1145.56	10.63	553.2	13.31	−119.07	−8.78

AC is area change; WSC is water storage change.

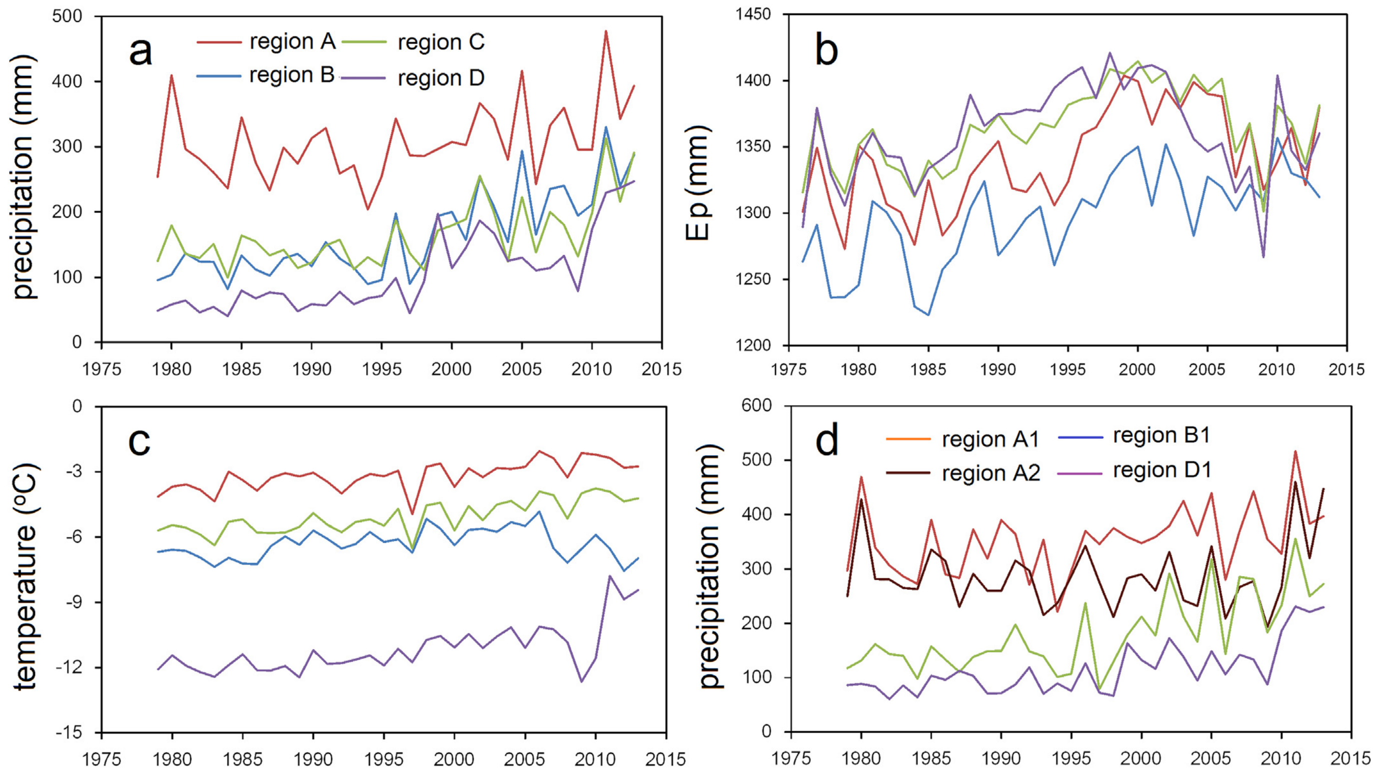

Fig. 6. Climate change parameters (precipitation, temperature and Ep) among the different study regions over the past few decades.

To more effectively analyze the origins of the variations among the lakes, we classified four sub-regions, namely, A1, A2, B1 and D1 (Fig. 4a), according to their different change types. The precipitation amounts in regions A1 and B1 showed trends similar to those of regions A and B, respectively, but region A2 exhibited a decreasing trend and region D1 had a slightly increasing trend from 1979 to 2013 (Fig. 6d).

3.4. Characteristics of lake surface area and water storage changes

As shown in Fig. 7, we separated all of the lakes into seven categories based on their size: 10–20 km^2 (91), 20–30 km^2 (36), 30–40 km^2 (28), 40–50 km^2 (19), 50–100 km^2 (60), 100–200 km^2 (42), and > 200 km^2 (39). The total areas of the > 200 km^2, 100–200 km^2 and 50–100 km^2 categories were 24,390.9 km^2, 5578.9 km^2 and 4336.2 km^2, respectively, in 2013, which collectively constituted 89.6% of the total area (38,292.6 km^2); these lakes increased by 4252.4 km^2 from 2000 to 2013 to occupy 85.1% of the total change in the area (4997 km^2) (Fig. 7a). The total area of the < 50 km^2 category was 3986.7 km^2 in 2013, which occupied only 10.4% of the total area, these lakes increased by 744.6 km^2 which occupied 14.9% of the total change in the lake surface area. As shown in Fig. 7b, the water storage increases in the > 200 km^2 category accounted for 67.5% of the total water storage increase from 2000 to 2013, and those in the 100–200 km^2 and 50–100 km^2 category constituted 12.4% and 11.4%, respectively, with the three categories of water storage increases occupying 91.3% of the total variation in water storage. The increasing areas in the > 200 km^2 category occupied 55.27% of the total increased area, and the increased water storage occupied 67.5% of the total increased water storage.

The water storage changes were mainly concentrated in the larger lakes (> 50 km^2), which constituted 91.3% of the total variation in the water storage, indicating that water storage changes in the larger lakes played a dominant role on the overall total lake storage change.

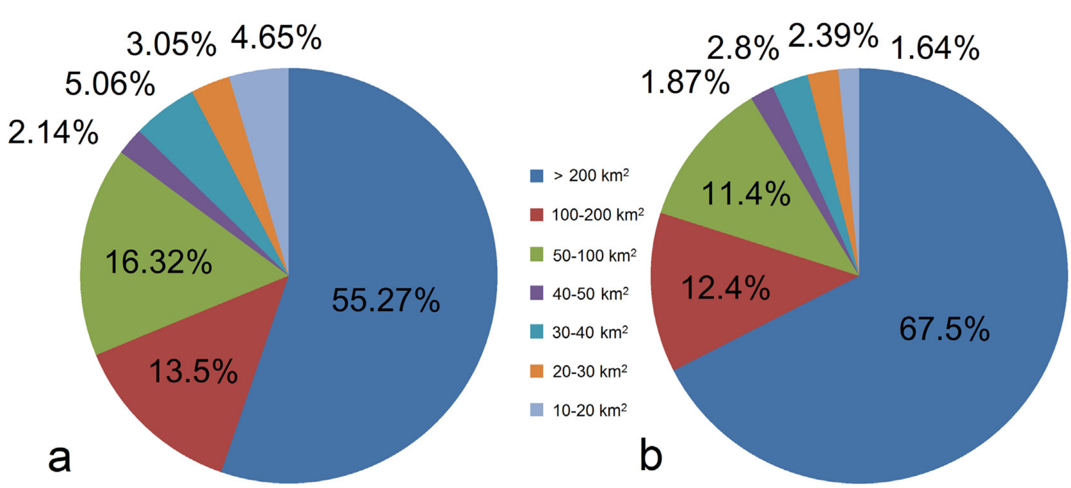

Fig. 7. The percentage of lake surface area change (a) and water storage change (b) to the total change throughout the TP for different lake sizes from 2000 to 2013.

Meanwhile, the water storage variation in the smaller lakes was insignificant in the overall storage variation throughout the TP. Water storage changes throughout most of the lakes (> 10 km^2) were calculated, but some of the smaller lakes were not included in the calculation of the water storage changes due to complex topography. Thus, we think that the total 315 lakes could represent the lake water storage change in the endorheic basins of the TP. That would be consistent with several of our findings. Although the total areas of region A and C increased by 100.9 km^2 and 8.63 km^2 from 1976 to 1990, the water storage decreased by 3.02 Gt and 0.49 Gt, respectively. Even though the increase in the lake surface area of region B was much more (1981.6 km^2) than that in region A (1869.1 km^2) from 2000 to 2013, the increase in the water storage in region A (59.02 Gt) was twice that in region B (29.74 Gt). Thirty-five large lakes (> 100 km^2) were observed in region A with an average area of 397.6 km^2 in 2013, including Selin Co (2397.4 km^2) and Nam Co (2020.9 km^2). However, only 19 large lakes (> 100 km^2) with an average area of 302.8 km^2 were observed in region B, wherein the largest and second-largest lake surface areas were 984.8 km^2 and 647.5 km^2, respectively. Accordingly, region A had larger lakes, and the lakes were more numerous than in region B (Fig. 1). These results indicate that variations in the lake surface area cannot represent the degree of lake change due to difference in the topography and lake size, but variations in the water storage can truly reflect changes in the lake.

3.5. The link between lake expansion and mass increases derived from GRACE

GRACE gravity data have been widely used to estimate terrestrial water storage changes (Haile, 2011; Jacob et al., 2012; Matsuo and Heki, 2010; Xiang et al., 2016; Yi and Sun, 2014; Zhong et al., 2009). The rate of mass increase throughout Tibet and the Qilian Shan was 7 ± 7 Gt/y during 2003–2010 based on the GRACE data (Jacob et al., 2012). A calculation of the change in the lake water storage using the same boundaries to Jacob et al. (2012) showed that the increased water storage rate was 7.19 Gt/y during 2000–2013 and that an increased lake water storage could effectively explain the mass increase throughout Tibet and the Qilian Shan. The results of Song et al. (2013) and Zhang et al. (2013b) also indicated that estimates of lake water storage changes are consistent with increased mass estimates derived from GRACE data over the TP. Thus, based on the above results, lake expansion could be the main reason for the increased mass throughout the TP. However, a comparison of the spatial distribution of lake water storage changes with the results derived from GRACE (Jacob et al., 2012; Song et al., 2013; Xiang et al., 2016), found inconsistencies among the regions exhibiting increased mass and water storage. The increased mass, which was estimated using GRACE, was mainly concentrated in the western sectors of regions B and C and was far greater than that increase in region A, but the increased lake water storage in regions B and C was far less than that in region A (Fig. 4). The lake water storage around Selin Co and Nam Co showed especially strong increases in region A, but the mass derived from GRACE showed only minor increases according to the results of Song et al. (2013) and Xiang et al. (2016). These results were perhaps coincidental, as the increase in the mass was similar to the increase in the lake water storage. Thus, lake expansion may not have been the main reason for the increased mass derived from the GRACE data.

4. Discussions

4.1. Analyzing the potential reasons for lake expansion with climate elements

Decreasing quantities of precipitation in region A and low precipitation amounts in the other three regions during 1976–1990 were perhaps the reason for the observed lake shrinkage, and high evaporation rate would have also limited lake expansion. However, for region A1 (Fig. 6d), the precipitation maintained significant variations at high magnitudes (334 mm), which was much higher than the average precipitation in region A (290 mm) (Fig. 6a). Thus, high precipitation may have been the cause of lake expansion during that period. Subsequent to 1990, the precipitation throughout the four regions maintained a significant and steadily increasing trend, and an increasing evaporation rate likely limited lake expansion. Therefore, increasing precipitation may have been the source of lake expansion during 1990–2000. The Ep showed a decreasing trend after 2000 and could have had a positive influence on the expansion of lakes throughout the TP, but precipitation was perhaps the main reason for the lake expansion, which continued to increase and was maintained at a high level. After 2000, increasing quantities of high-level precipitation were likely the main source of lake expansion. Four small regions were consequently analyzed (Fig. 6d). For region A2, the precipitation continued to decrease until 2010, but the lakes expanded after 2000. Large numbers of glaciers are distributed throughout region A2, and thus, increased amounts of glacial meltwater were perhaps the main reason for lake expansion subsequent to 2000, which were coincident with rising temperatures. For region B1, the precipitation maintained a steadily low level until 2000 and may have been the reason for lake shrinkage during 1976–2000, after which the lakes expanded coincident with rising precipitation amounts after 2000. The precipitation quantity demonstrated a good relationship with the lake changes, which showed a similar trend in these changes.

As shown in Fig. 5b, the Ep increased from 1976 to 2000 and then decreased from 2000 to 2013. This trend is basically consistent with that of the lake variations, indicating the Ep was not the main reason for the lake change. Increasing Ep limited lake expansion during 1976–1990, and decreasing Ep imposed a positive influence on lake expansion. The average rates of lake level rise during 2000–2013 in regions A, C and D were 265 mm/y, 186 mm/y and 321 mm/y, respectively, which were determined via rough estimates. Thus, decreasing Ep contributed approximately 1.5%, 2.5% and 1.7% to lake expansion. However, the average annual temperature rose from 1979 to 2013 (Fig. 6c), and previous studies indicated that glaciers throughout TP have experienced serious shrinkage in recent decades (Neckel et al., 2014; Yao et al., 2012). Thus, increases in glacial meltwater with rising temperature may constitute an important contribution to lake expansion on the TP.

According to the above results, precipitation was perhaps the main reason for lake change throughout the TP, and glacial meltwater coincident with rising temperature also may have been an important contributor in the regions with large amounts of glaciers distribution. Continuously decreasing precipitation caused lake shrinkage in region A2 during 1976–2000, but these lakes started to expand with decreasing precipitation and increasing Ep after 2000, and thus, increased glacial meltwater with rising temperature may have made these lakes expand. Low precipitation in regions B, C and D, which were located in much colder and drier climates than region A, were the cause of lake shrinkage during 1976–1990, but both increased glacial meltwater and increased precipitation may have constituted an important contribution to lake expansion, especially in those lakes located in the extremely cold and dry region D. Increasing precipitation may have been evaporated but was not expelled into runoff in the arid climate of region D, which showed the lowest precipitation and highest Ep. Thus, glacial meltwater may have been the main reason for lake expansion in region D. Decreasing precipitation and increasing Ep may have been the reason for lake shrinkage in region E, and hydropower stations perhaps exhibited strong influences on the lake shrinkage of Yamzho Yumco.

4.2. Contribution of glacial meltwater to lake expansion

According to the second Chinese glacier inventory which was interpreted based on Landsat TM/ETM + images during 2006–2010 (Guo

et al., 2015), the glacier areas of regions A, B, C and D were 1809.1 km^2, 2130.6 km^2, 633 km^2 and 2711.4 km^2, respectively. The glacier area of region C was the least among these four regions. Most of the glaciers over the TP have experienced serious shrinkage coincident with rising temperatures over recent decades (Bolch et al., 2010, 2012; Ke et al., 2015; Neckel et al., 2014; Wei et al., 2014; Yao et al., 2012). The rate of retreat for glaciers in region A (8.6–36.38%) was faster than those in regions B and C (2.48–6.52%) from the 1970s to 2009, and in region D, the rate of retreat was 2.76–10.36% (Wei et al., 2014). Glacial meltwater made an important contribution to the lake expansion of Selin Co, Nam Co and Pung Co, accounting for 11.7%, 28.7% and 11.4%, respectively, of the total rise in lake levels based on modern mass balance measurements (Lei et al., 2013). Glacial meltwater accounted for 14–30% of the total runoff for Nam Co, Tangra Yumco, Mapam Yumco and Peiku Co basin based on modeling and remote sensing data (Biskop et al., 2016). Glacial meltwater may have made an equivalent contribution to lake expansion as precipitation/evaporation in the Tanggula Mountains and the western TP (Qiao and Zhu, 2017; Song and Sheng, 2016). The results of Zhu et al. (2010) indicated that, although precipitation was the main inflow component for Nam Co, increased glacial meltwater was the main reason for lake expansion. In conclusion, glacial meltwater may play an important role on the expansion of lakes on the TP.

However, if the water storage change from lake expansion were from glacial meltwater, and since the water storage of region A increased by 59.02 Gt (4.54 Gt/y) from 2000 to 2013, the average thickness of the glaciers would have thinned at a rate of 2.5 m/y water equivalent (w.e.) for a total glacier area of 1809.1 km^2. The same calculations for the glaciers in regions B, C and D reveal values of 1.4 m/y w.e., 1.1 m/y w.e. and 0.4 m/y w.e.. According to the results of in situ mass balance observations (Table 3), Zhadang glacier, which supplies glacial meltwater to Nam Co, shrank at a rate of −0.59 m/y from 2005 to 2008 (Yao et al., 2010), while the thinning rates for Zhongxi glacier and Gurehekou glacier were −0.523 m/y from 2007 to 2009 and −0.312 m/y from 2005 to 2009, respectively, (Yao et al., 2012). These three glaciers are located in the Nyainqentanglha Mountains. The thinning rate of Xiaodongkemadi glacier was −0.549 m/y from 2005 to 2009 in the Tanggula Mountains. The Chhota Shigri glacier shrank by −0.667 m/y from 2000 to 2009 in the western Himalayas (Azam et al., 2012). These last five glaciers are located in region A or in the surrounding areas, and the average mass balance of these five glaciers was −0.618 m/y or approximately −0.557 m/y w.e. If we take these results (−0.455 m/y w.e.) as an average for the four regions, glacial meltwater could have accounted for 22.2%, 39.8%, 50.6% and 100% of the water storage changes in regions A, B, C and D, respectively. Serious glacier shrinkage has mainly occurred in the Himalayas (Table 3), for example, the shrinkage rate for the four glaciers of Parlung ranged from −0.781 m/y to −1.698 m/y in the southeastern TP. Thus, increased glacial meltwater made important contributions to lake expansion in region A and was perhaps the main source of lake expansion in the extremely cold and dry region D, throughout which large amounts of glaciers are distributed. The significance of glacial meltwater on lake expansion was much stronger in regions B, C and D relative to region A, which was located in an area with high precipitation and low Ep conditions.

5. Conclusions

A total of 315 lakes (> 10 km^2) throughout the endorheic basins of the TP were investigated based on SRTM DEM data and Landsat images. The overall lake surface area expanded from 31,858 km^2 in 1976 to 38,292.6 km^2 in 2013. Most of the lakes showed a shrinking trend during the period 1976–1990, after which most of the lakes expanded, but the lakes in the southern part of the TP (region E) still shrank. The water storage changes were estimated based on the SRTM data, which provided the topography surrounding the lakes. The total water storage decreased by 23.69 Gt from 1976 to 1990 and then increased by 140.8 Gt from 1990 to 2013. Increasing lake water storage was mainly concentrated in the central and northern part of the TP (region A and B). The water storage change in region A constituted 53.75% of the total water storage change during 2000–2013, and larger lakes (> 50 km^2) played a dominant role in the overall variation in the water storage (91.3% of total change). The increase in the lake surface area from 2000 to 2013 in region B (1981.6 km^2) was greater than that in region A (1869.1 km^2), but the increase in the water storage change (29.74 Gt) was only one-half of that in region A (59.02 Gt). These results indicate that the variation in the lake surface area change cannot represent the degree of lake change due to differences in the topography and lake size.

Although the total lake water storage change showed good coincidence with the increased mass derived using GRACE data, the spatial distribution of those variations showed large differences. This indicates the complexity of land surface water balance in different water sheds due to the other signals included within the GRACE (e.g., soil moisture and groundwater). Based on modern mass balance observation data, glacial meltwater perhaps constituted the contributions of 22.2%, 39.8%, 50.6% and 100% to the increased water storage in regions A, B, C and D during 2000–2013 by rough estimates. Decreasing and low precipitation in the other three regions were the main reason for the shrinking of lakes during 1976–1990. High precipitation and low Ep were the main reason for the lake expansion and glacial meltwater was an important contributor to the lakes of region A1, and glacial meltwater was the main reason for lake expansion in region A2 after 2000. Increasing precipitation and glacial meltwater were perhaps the major reason for lake expansion in regions B and C after 1990. However, glacial meltwater could also have been a primary contributor to lake

Table 3
Recent glacier mass balance measurement in the TP and surrounding.

Glacier	Latitude(N)	Longitude (E)	Area (km^2)	Mass balance (m/yr)	Date	Locations	Source
Zhadang	30.476	90.645	1.98	−0.59	2005–2008	Nyainqentanglha Mountain	Yao et al. (2010)
Gurenhekou	30.183	90.467	1.4	−0.312	2005–2009	Nyainqentanglha Mountain	Yao et al. (2012)
Zhongxi	30.867	91.45	1.6	−0.523	2007–2009	Nyainqentanglha Mountain	Yao et al. (2012)
Kangwure	28.467	85.817	1.9	−0.66	2005–2009	Central Himalayas	Yao et al. (2012)
AX010	27.7	86.567	0.4	−0.81	2005	Central Himalayas	Fujita and Nuimura (2011)
Yala	28.233	85.617	1.9	−0.8	2005	Central Himalayas	Fujita and Nuimura (2011)
Naimona'nyi	30.45	81.333	7.8	−0.556	2005–2009	West Himalayas	Yao et al. (2012)
Hamtah	32.35	81.5		−1.501	2003–2005	West Himalayas	Haeberli et al. (2009)
Chhota Shigri	32.2	81.5	15.7	−0.667	2000–2009	West Himalayas	Azam et al. (2012)
Xiaodongkemadi	33.167	92.133	1.8	−0.549	2005–2009	Tanggula Mountain	Yao et al. (2012)
Parlung No.10	29.283	96.9	2.1	−0.781	2005–2008	Southeast TP	Yao et al. (2012)
Parlung No.12	29.3	96.9	0.2	−1.698	2005–2009	Southeast TP	Yao et al. (2012)
Parlung No.94	29.38333	96.98333	2.5	−0.922	2005–2009	Southeast TP	Yao et al. (2012)
Parlung No.390	29.35	97.01667	0.5	−1.019	2006–2009	Southeast TP	Yao et al. (2012)

expansion in region D, which was located in an extremely cold and dry climate with a broad distribution of glaciers.

Acknowledgements

We thank the editor, associate editor and anonymous reviewers whose suggestions and comments were very helpful in improving this manuscript. This work is supported by the CAS Strategic Priority Research Program (XDA20020100), NSFC project (41831177); CAS International Partnership Program (131C11KYSB20160061), and the 13th Five-year Informatization Plan of Chinese Academy of Sciences (XXH13505-06). The surface meteorological data were provided by the Center of Science Data on the Tibetan Plateau (http://www.tpedatabase.cn).

References

Azam, M.F., Wagnon, P., Ramanathan, A., Cincent, C., Sharma, P., Arnaud, Y., Linda, A., Pottakkal, J.G., Chevallier, P., Singh, V.B., 2012. From balance to imbalance: a shift in the dynamic behaviour of Chhota Shigri glacier, western Himalaya, India. J. Glaciol. 58 (208), 315–324.

Biskop, S., Maussion, F., Krause, P., Fink, M., 2016. Differences in the water-balance components of four lakes in the southern-central Tibetan Plateau. Hydrol. Earth Syst. Sci. 20 (1), 209–225.

Bolch, T., Yao, T., Kang, S., Buchroithner, M.F., Scherer, D., Maussion, F., Huintjes, E., Schneider, C., 2010. A glacier inventory for the western Nyainqentanglha Range and the Nam Co Basin, Tibet, and glacier changes 1976–2009. Cryosphere 4 (3), 419–433.

Bolch, T., Kulkarni, A., Kaab, A., Huggel, C., Paul, F., Cogley, J.G., Frey, H., Kargel, J.S., Fujita, K., Scheel, M., Bajracharya, S., Stoffel, M., 2012. The state and fate of Himalayan glaciers. Science 336, 310–314.

Chen, Y., Yang, K., He, J., Qin, J., Shi, J., Du, J., He, Q., 2011. Improving land surface temperature modeling for dry land of China. J. Geophys. Res. 116, D20104.

Fujita, K., Nuimura, T., 2011. Spatially heterogeneous wastage of Himalayan glaciers. Proc. Natl. Acad. Sci. U. S. A. 108 (34), 14011–14014.

Gao, B., 1996. NDWI - a normalized difference water index for remote sensing of vegetation liquid water from space. Remote Sens. Environ. 58 (3), 257–266.

Guo, W., Liu, S., Xu, J., Wu, L., Shangguan, D., Yao, X., Wei, J., Bao, W., Yu, P., Liu, Q., Jiang, Z., 2015. The second Chinese glacier inventory: data, methods and results. J. Glaciol. 61 (226), 357–372.

Haeberli, W., Gärtner-Roer, I., Hoelzle, M., Paul, F., Zemp, M.G., 2009. Glacier Mass Balance Bulletin No. 10 (2006–2007). IAHS (ICSI), Zürich.

Haile, K.H., 2011. Estimation of Terrestrial Water Storage in the Upper Reach of Yellow River (MSc Thesis). University of Twente, Netherlands, pp. 7–11.

He, J., Yang, K., 2011. China Meteorological Forcing Dataset. Cold and Arid Regions Science Data Center at Lanzhou, China.

Huffman, G., Adler, R., Bolvin, D., Gu, G., Nelkin, E., Bowman, K., Hong, Y., Stocker, E., Wolff, D., 2007. The TRMM multisatellite precipitation analysis (TMPA): quasi-global, multiyear, combined-sensor precipitation estimates at fine scales. J. Hydrometeorol. 8, 38–55.

Jacob, T., Wahr, J., Pfeffer, W.T., Swenson, S., 2012. Recent contributions of glaciers and ice caps to sea level rise. Nature 482 (7368), 514–518.

Jiang, L., Nielsen, K., Andersen, O., Bauer-Gottwein, 2017. Monitoring recent lake level variations on the Tibetan Plateau using Cryosat-2 SARIn mode data. J. Hydrol. 544, 109–124.

Ke, L., Ding, X., Song, C., 2015. Estimation of mass balance of Dongkemadi glaciers with multiple methods based on multi-mission satellite data. Quat. Int. 371, 58–66.

Lehner, B., Verdin, K., Jarvis, A., 2008. New global hydrography derived from spaceborne elevation data. Eos. Trans. AGU 89 (10), 93–94.

Lei, Y., Yao, T., Bird, B.W., Yang, K., Zhai, J., Sheng, Y., 2013. Coherent lake growth on the central Tibetan Plateau since the 1970s: characterization and attribution. J. Hydrol. 483 (3), 61–67.

Lei, Y., Yao, T., Yang, K., Sheng, Y., Kleinherenbrink, M., Yi, S., Bird, B.W., Zhang, X., Zhu, L., Zhang, G., 2017. Lake seasonality across the Tibetan Plateau and their varying relationship with regional mass changes and local hydrology. Geophys. Res. Lett. 44 (2), 892–900.

Li, Y., Liao, J., Guo, H., Liu, Z., Shen, G., 2014. Patterns and potential drivers of dramatic changes in Tibetan lakes, 1972–2010. PLoS One 9, e111890.

Liu, J., Xie, Z., 2013. Improving simulation of soil moisture in China using a multiple meteorological forcing ensemble approach. Hydrol. Earth Syst. Sci. 17 (9), 3355–3369.

Liu, J., Wang, S., Yu, S., Yang, D., Zhang, L., 2009. Climate warming and growth of high-elevation inland lakes on the Tibetan Plateau. Glob. Planet. Chang. 67 (3–4), 209–217.

Ma, N., Szilagyi, J., Niu, G.Y., Zhang, Y., Zhang, T., Wang, B., Wu, Y., 2016. Evaporation variability of Nam Co lake in the Tibetan Plateau and its role in recent rapid lake expansion. J. Hydrol. 537, 27–35.

Matsuo, K., Heki, K., 2010. Time-variable ice loss in Asian high mountains from satellite gravimetry. Earth Planet. Sci. Lett. 290 (1–2), 30–36.

McFeeters, S., 1996. The use of the Normalized Difference Water Index (NDWI) in the delineation of open water features. Int. J. Remote Sens. 17 (7), 1425–1432.

McMahon, T., Peel, M., Lowe, L., Srikanthan, R., McVicar, T., 2013. Estimating actual, potential, reference crop and pan evaporation using standard meteorological data: a pragmatic synthesis. Hydrol. Earth Syst. Sci. 17 (4), 1331–1363.

Neckel, N., Kropáček, J., Bolch, T., Hochschild, V., 2014. Glacier mass changes on the Tibetan Plateau 2003–2009 derived from ICESat laser altimetry measurements. Environ. Res. Lett. 9, 014009.

Penman, H., 1948. Natural evaporation from open water, bare soil and grass. Proc. R. Soc. Lond. 193, 120–145.

Phan, V.H., Lindenbergh, R.C., Menenti, M., 2013. Geometric dependency of Tibetan lakes on glacial runoff. Hydrol. Earth Syst. Sci. 17 (10), 4061–4077.

Qiao, B., Zhu, L., 2017. Differences and cause analysis of changes in lakes of different supply types in the northwestern Tibetan Plateau: difference and cause analysis of lakes change. Hydrol. Process. 31 (15), 2752–2763.

Qiao, B., Zhu, L., Wang, J., Ju, J., Ma, Q., Liu, C., 2017. Estimation of lakes water storage and their changes on the northwestern Tibetan Plateau based on bathymetric and Landsat data and driving force analyses. Quat. Int. 454, 56–67.

Rodriguez, E., Morris, C.S., Belz, J.E., 2006. A global assessment of the SRTM performance. Photogramm. Eng. Remote. Sens. 72 (3), 249–260.

Sheffield, J., Goteti, G., Wood, E.F., 2006. Development of a 50-year high-resolution global dataset of meteorological forcings for land surface modeling. J. Clim. 19 (13), 3088–3111.

Song, C., Sheng, Y., 2016. Contrasting evolution patterns between glacier-fed and non-glacier-fed lakes in the Tanggula Mountains and climate cause analysis. Clim. Chang. 135 (3–4), 493–507.

Song, C., Huang, B., Ke, L., 2013. Modeling and analysis of lake water storage changes on the Tibetan Plateau using multi-mission satellite data. Remote Sens. Environ. 135 (4), 25–35.

Song, C., Huang, B., Richards, K., Ke, L., Phan, V., 2014. Accelerated lake expansion on the Tibetan Plateau in the 2000s: induced by glacial melting or other processes? Water Resour. Res. 50 (4), 3170–3186.

Wan, W., Xiao, P., Feng, X., Li, H., Ma, R., Duan, H., Zhao, L., 2014. Monitoring lake changes of Qinghai-Tibetan Plateau over the past 30 years using satellite remote sensing data. Chin. Sci. Bull. 59 (10), 1021–1035.

Wan, W., Long, D., Hong, Y., Ma, Y., Yuan, Y., Xiao, P., Duan, H., Han, Z., Gu, X., 2016. A lake data set for the Tibetan Plateau from the 1960s, 2005, and 2014. Sci. Data 3, 160039.

Wang, X., Gong, P., Zhao, Y., Xu, Y., Cheng, X., Niu, Z., Luo, Z., Huang, H., Sun, F., Li, X., 2013. Water-level changes in China's large lakes determined from ICESat/GLAS data. Remote Sens. Environ. 132, 131–144.

Wei, J., Liu, S., Guo, W., Yao, X., Xu, J., Bao, W., Jiang, Z., 2014. Surface-area changes of glaciers in the Tibetan Plateau interior area since the 1970s using recent Landsat images and historical maps. Ann. Glaciol. 55 (66), 213–222.

Wu, Y., Zheng, H., Zhang, B., Chen, D., Lei, L., 2014. Long-term changes of lake level and water budget in the Nam Co Lake Basin, Central Tibetan Plateau. J. Hydrometeorol. 15 (3), 1312–1322.

Xiang, L., Wang, H., Steffen, H., Wu, P., Jia, L., Jiang, L., Shen, Q., 2016. Groundwater storage changes in the Tibetan Plateau and adjacent areas revealed from GRACE satellite gravity data. Earth Planet. Sci. Lett. 449, 228–239.

Xu, Z., Gong, T., Li, J., 2008. Decadal trend of climate in the Tibetan Plateau-regional temperature and precipitation. Hydrol. Process. 22 (16), 3056–3065.

Yang, W., Yao, T., Guo, X., Zhu, M., Li, S., Kattel, D.B., 2013. Mass balance of a maritime glacier on the southeast Tibetan Plateau and its climatic sensitivity. J. Geophys. Res. Atmos. 118 (17), 9579–9594.

Yang, W., Guo, X., Yao, T., Zhu, M., Wang, Y., 2016. Recent accelerating mass loss of southeast Tibetan glaciers and the relationship with changes in macroscale atmospheric circulations. Clim. Dyn. 47 (3–4), 805–815.

Yang, R.M., Zhu, L.P., Wang, J.B., Ju, J.T., Ma, Q.F., Turner, F., Guo, Y., 2017. Spatiotemporal variations in volume of closed lakes on the Tibetan Plateau and their climatic responses from 1976 to 2013. Clim. Chang. 140 (3–4), 621–633.

Yao, T.D., Li, Z., Yang, W., Guo, X., Zhu, L., Kang, S., Yu, W., 2010. Glacial distribution and mass balance in the Yarlung Zangbo river and its influence on lakes. Chin. Sci. Bull. 55 (20), 2072–2078.

Yao, T.D., Thompson, L., Yang, W., Yu, W.S., Gao, Y., Guo, X.J., Yang, X.X., Duan, K.Q., Zhao, H.B., Xu, B.Q., Pu, J.C., Lu, A.X., Xiang, Y., Kattel, D.B., Joswiak, D., 2012. Different glacier status with atmospheric circulations in Tibetan Plateau and surroundings. Nat. Clim. Chang. 2 (9), 663–667.

Yao, X., Li, L., Zhao, J., Sun, M., Li, J., Gong, P., An, L., 2015. Spatial-temporal variations of lake ice in the Hoh Xil region from 2000 to 2011. Acta Geograph. Sin. 70 (7), 1114–1124.

Yi, S., Sun, W.K., 2014. Evaluation of glacier changes in high-mountain Asia based on 10 year GRACE RL05 models. J. Geophys. Res. Solid Earth 119 (3), 2504–2517.

Zhang, B., Wu, Y., Zhu, L., Wang, J., Li, J., Chen, D., 2011a. Estimation and trend detection of water storage at Nam Co Lake, central Tibetan Plateau. J. Hydrol. 405 (1–2), 161–170.

Zhang, G., Xie, H., Kang, S., Yi, D., Ackley, S.F., 2011b. Monitoring lake level changes on the Tibetan Plateau using ICESat altimetry data (2003–2009). Remote Sens. Environ. 115 (7), 1733–1742.

Zhang, G., Xie, H., Yao, T., Kang, S., 2013a. Water balance estimates of ten greatest lakes in China using ICESat and Landsat data. Chin. Sci. Bull. 58 (31), 3815–3829.

Zhang, G., Yao, T., Xie, H., Kang, S., Lei, Y., 2013b. Increased mass over the Tibetan Plateau: from lakes or glaciers? Geophys. Res. Lett. 40 (10), 2125–2130.

Zhang, G., Yao, T., Xie, H., Zhang, K., Zhu, F., 2014. Lakes' state and abundance across the Tibetan Plateau. Chin. Sci. Bull. 59 (24), 3010–3021.

Zhang, G., Yao, T., Shum, C.K., Yi, S., Yang, K., Xie, H., Feng, W., Bolch, T., Wang, L., Behrangi, A., Zhang, H., Wang, W., Xiang, Y., Yu, J., 2017. Lake volume and groundwater storage variations in Tibetan Plateau's endorheic basin. Geophys. Res.

Lett. 44, 5550–5560.
Zhong, M., Duan, J.B., Xu, H.Z., Peng, P., Yan, H.M., Zhu, Y.Z., 2009. Trend of China land water storage redistribution at medi- and large-spatial scales in recent five years by satellite gravity observations. Chin. Sci. Bull. 54 (5), 816–821.
Zhou, J., Wang, L., Zhang, Y., Guo, Y., Li, X., Liu, W., 2016. Exploring the water storage changes in the largest lake (Selin Co) over the Tibetan Plateau during 2003–2012 from a basin-wide hydrological modeling. Water Resour. Res. 51, 8060–8086.
Zhu, L., Xie, M., Wu, Y., 2010. Quantitative analysis of lake area variations and the influence factors from 1971 to 2004 in the Nam Co basin of the Tibetan Plateau. Chin. Sci. Bull. 55 (13) (1294-130).